Modeling of electrode polarization for electrolytic cells with a limited ionic adsorption

Atsushi Sawada
Advanced Technologies Research and Developments, Merck Ltd., Aikawa, Kanagawa 243-0303, Japan
(Received 17 June 2013; published 18 September 2013)

Dilute electrolytic cells filled with chlorobenzene containing small amounts of tetrabutylammonium tetraphenylborate show anomalous dielectric dispersions in low-frequency regions. We propose a new model for electrode polarization in order to analyze the dielectric behavior of the dilute electrolytic cells. The model comprises two capacitive components: One is the space-charge polarization accompanied with a specific ionic adsorption on electrodes, and the other is the electrode capacitance which is brought about by an electronic spillover from the electrode surface. This model can primarily explain the anomalous frequency-dependent dielectric behavior of the electrolytic cells not only with low electrolyte concentrations, but also with high concentrations and can correctly describe the characteristics of the electrode polarization reflected in the dielectric spectra.

DOI: 10.1103/PhysRevE.88.032406 PACS number(s): 66.10.−x, 77.22.−d, 82.45.−h

I. INTRODUCTION

Dielectric spectroscopy is a powerful tool not only for analyzing the molecular polarization performance of materials, but also for characterizing mobile ions contained in the materials as impurities [1–7]. The polarization of the mobile ions at electrodes is the so-called space-charge polarization, and its dielectric effect is brought about by the generation of a macroscopic dipole that is represented by the displacement of average positions of positive and negative ions under the influence of an externally applied electric field [1,8,9]. The theoretical calculation for the space-charge polarization is performed by solving the Poisson-Nernst-Planck (PNP) equation under an ac electric field application [10–15]. The equation of the complex dielectric constant obtained by the calculation includes the diffusion coefficient and the number density of the mobile ions as parameters, and thus, these parameters can be determined by fitting the calculated values to observed values on the dielectric spectrum. An essential point in the theoretical calculation of the space-charge polarization is to consider the influence of external charges on the internal electric field formation, and the influence can be quantitatively taken into account by including the contribution of the space-charge polarization in the dielectric constant of Poisson's equation [9,16–18].

In actual cases, the behavior of ions on the electrode is complicated, and thus, the dielectric spectra observed for dilute electrolytic cells in low-frequency regions are not fully explained by the conventional formula of the space-charge polarization. The space-charge polarization usually exhibits a dielectric relaxation in a low-frequency region below kilohertz order, and its characteristic is somewhat different from that of Debye-type dielectric relaxation [9]. On the other hand, another dielectric relaxation, that is, the Debye-type one, is sometimes observed, and the two types of dielectric relaxations show different cell thickness dependences for their relaxation frequencies [4,9]. If the two types of dielectric relaxations overlap in the same frequency range, the analysis of the dielectric spectrum becomes complicated.

Although the contribution of the space-charge polarization to the complex dielectric constant has been studied theoretically and the dielectric spectrum observed in a specific frequency region for a dilute electrolytic cell has been well explained by using the theory [9,18], another dielectric relaxation, that usually appears in lower frequencies, has not been discussed fully, and no persuasive theoretical model has been established. The origin of the dielectric relaxation in the lower frequencies is presumed to be related to the specific adsorption of ions on the electrodes; nevertheless, the existing model of the space-charge polarization considering the ionic adsorption cannot explain the experimental results for dilute electrolytic solutions [19]. One of the reasons for the failure is that the effect of external charges for internal electric field formation is not taken into account on the calculation of the space-charge polarization in the existing model.

In the present paper, we calculate the PNP equation under the boundary condition in accordance with the specific ionic adsorption on the electrode. The effect of the external charges for internal field formation is taken into account for calculating the PNP equation. It is known that metal electrodes exhibit electronic spillovers on their surfaces and restrict the closest distances that ions can approach [20,21]. This effect is also considered for analyzing the experimental results. A new model of the electrode polarization is, thus, built by combining the space-charge polarization and the electrode capacitance due to the electronic structure of the electrode surface.

II. ANALYTICAL TREATMENT OF ELECTRODE POLARIZATION AND SIMULATION OF A DIELECTRIC SPECTRUM

A. Space-charge polarization in the absence of ionic adsorption on the electrode

Let us consider a parallel-plate cell filled with a uniunivalent electrolyte solution, the distance of which between electrodes is d. Assume that the electrolyte is completely dissociated, and the positive and negative ions are distributed uniformly in the slab of the solution in the absence of an external electric field. The model considered here does not account for "native" charges on the electrodes that would give a nonuniform ionic distribution at the zero applied potential. We restrict our consideration to a one-dimensional case with the transport of the mobile ions in the x direction under an electric field applied

externally. Let $p(x,t)$ and $n(x,t)$ be the number densities of the positive and negative ions, respectively, at position x and time t. Considering the experimental system in the present paper, we assume that the diffusion coefficient of the positive ions is equal to that of the negative ions; similarly, the mobility of the positive ions is equal to that of the negative ions. Thus, let D and μ be the diffusion coefficient and the mobility of the positive or negative ions, respectively. Current densities for the positive and negative ions $j_p(x,t)$ and $j_n(x,t)$ under the electric field $E(x,t)$ reduce to

$$j_p(x,t) = q\mu p(x,t)E(x,t) - qD\,\partial p(x,t)/\partial x, \tag{1}$$

and

$$j_n(x,t) = q\mu n(x,t)E(x,t) + qD\,\partial n(x,t)/\partial x, \tag{2}$$

where q is the elementary charge. The continuity equations are written as

$$q\,\partial p(x,t)/\partial t = -\partial j_p(x,t)/\partial x, \tag{3}$$

and

$$q\,\partial n(x,t)/\partial t = \partial j_n(x,t)/\partial x. \tag{4}$$

Thus, we obtain

$$\partial p(x,t)/\partial t = D\,\partial^2 p(x,t)/\partial x^2 - \mu\partial[p(x,t)E(x,t)]/\partial x, \tag{5}$$

and

$$\partial n(x,t)/\partial t = D\,\partial^2 n(x,t)/\partial x^2 + \mu\partial[n(x,t)E(x,t)]/\partial x. \tag{6}$$

The internal electric field $E(x,t)$ is governed by Poisson's equation,

$$\partial E(x,t)/\partial x = q[p(x,t) - n(x,t)]/[\varepsilon_0\varepsilon_r(t)], \tag{7}$$

where $\varepsilon_r(t)$ is the relative dielectric constant of the electrolytic solution including the contribution of the space-charge polarization. $\varepsilon_r(t)$ varies with time [9,16–18]. Assuming that the voltage applied between the electrodes is $V(t)$, we also require that

$$V(t) = \int_0^d E(x,t)dx, \tag{8}$$

and

$$\int_0^d p(x,t)dx = \int_0^d n(x,t)dx. \tag{9}$$

Here, we assume that the motion of the positive and negative ions under the electric field is completely blocked at the electrodes but they do not adsorb on the electrodes. The boundary conditions can be written as

$$j_p(x,t) = q\mu p(x,t)E(x,t) - qD\,\partial p(x,t)/\partial x = 0, \tag{10}$$

and

$$j_n(x,t) = q\mu n(x,t)E(x,t) + qD\,\partial n(x,t)/\partial x = 0, \tag{11}$$

at $x = 0$ and $x = d$.

We will discuss the case in which a simple sinusoidal forcing voltage $V(t) = V_1\exp(i\omega t)$ is applied between the electrodes where $i = \sqrt{-1}$. Since Eqs. (5)–(11) are nonlinear, the current through the electrolytic solution will contain all harmonics of the forcing voltage, and accurate solutions for $p(x,t)$, $n(x,t)$, and $E(x,t)$ would show that they would all involve zero-frequency components with the fundamental and all its overtones. However, the ratio of higher harmonic components to the fundamental component in $p(x,t)$, $n(x,t)$, and $E(x,t)$ may be made negligible by taking V_1 to be sufficiently small. Thus, by providing such a small V_1, $p(x,t)$, $n(x,t)$, and $E(x,t)$ may be written in the form [10–13]

$$p(x,t) = p_0(x) + p_1(x)\exp(i\omega t), \tag{12}$$

where p_0 represents the number density of the positive ions in the absence of the external field. In the present model, we assume that the number density of positive ions is equal to that of negative ions in the absence of the external field, and thus, we set that $p_0 = n_0 = c_0$. Since no dc component is involved in the applied voltage, $E_0 = 0$.

Regarding the issue of which V_1 level is required for neglecting the higher harmonic components, one criterion may be that V_1 should be smaller than 0.025 V, that is known as the thermal voltage k_BT/q at room temperature [13], where k_B is the Boltzmann constant and T is the absolute temperature. Nevertheless, we have confirmed that the frequency-dependent curve of the complex dielectric constant due to the space-charge polarization observed for an electrolytic solution cell does not change significantly in the range of the applied ac voltage between 0.005 (rms) and 0.1 V (rms) and clear changes appear in the range over 0.1 V (rms) [22]. This experimental result agrees with the simulation result obtained in the author's previous paper [22] in which the frequency dependences of the complex dielectric constant are calculated with the applied ac voltages as a parameter.

We assume that the electric field within the electrolyte is homogeneous. This assumption of the electric field is an essential point for building the present model; therefore, here, we will reconfirm the validity of the approximation using the homogeneous field for analyzing the space-charge polarization. In the present paper, the dielectric property of the space-charge polarization is measured by employing a frequency response analyzer. A small ac voltage is applied to the electrolytic cell in the measurement, and the mobile ions in the cell are redistributed under the influence of the applied voltage. Since the internal electric field becomes inhomogeneous due to the ionic redistribution, it is necessary to solve Poisson's equation for determining the internal field accurately.

In the classical theory for analyzing the PNP equation [10–13], the contribution of the space-charge polarization is not included in the dielectric constant of Poisson's equation. The space-charge polarization is considered to be the formation of a macroscopic dipole in the electrolytic cell, and its magnitude is defined by the product of the elementary charge, the number density of ions, and the distance between the average positions of the positive and negative ions [1,8,9]. The space-charge polarization induces external charges on the electrodes of the electrolytic cell as in the case of the dipole, atomic, and electronic polarizations of the matrix material. Hence, the dielectric effect of the space-charge polarization must be considered for the dielectric constant of Poisson's equation for calculating the internal electric field. The external

charge on the electrode Q_{el} is expressed as $Q_{el} = \varepsilon_0 \varepsilon_r E_{el}$ providing that E_{el} is the electric field of the electrode. If the contribution of the space-charge polarization to Q_{el} is small enough compared with that of the dipole polarization of the matrix material, the contribution of the space-charge polarization can be neglected. However, the mobile ions, even in very small concentrations, give dominant contributions to Q_{el} as in the present electrolytic cells.

The internal electric fields of the electrolytic cell containing tetrabutylammonium tetraphenylborate (TBATPB) at the concentration of 500 ppb (parts per 10^9) have been calculated for the two cases: One is that the contribution of the space-charge polarization is included in the dielectric constant of Poisson's equation and the other is that the contribution of the space-charge polarization is not included [17]. The results show that the internal electric field draws a moderate hyperbolic curve between the two parallel electrodes for the former case, whereas, the internal electric field becomes so inhomogeneous for the latter case that the electric field is concentrated in the vicinity of the electrodes and the electric field of the other part becomes almost zero. Since the dielectric effect of the space-charge polarization is not considered in the latter case, the value of Q_{el} is underestimated in the calculation. The external (counter) charges on the electrodes electrically neutralize the mobile ions that reached the electrodes; hence, the quite inhomogeneous electric field near the electrode in the latter case is considered to be brought about by the underestimated value of Q_{el}. In Ref. [17], it is also shown that the frequency-dependent curve of the complex dielectric constant, calculated assuming the homogeneous field becomes very close to that assuming the hyperbolic field, and the Stokes radii of TBA^+ and TPB^- ions, obtained by analysis with the homogeneous field, are around 10% smaller than those by analysis with the hyperbolic field.

We have simulated the frequency-dependent curves of the complex dielectric constant using the classical theory of the space-charge polarization developed by Macdonald [12] and Friauf [13] and found that the increase in the dielectric constant at low frequencies is suppressed and the relaxation frequency shifts to the high-frequency side with increasing the number density of ions in the electrolytic cell [18]. However, such frequency-dependent behavior has not been observed in the dielectric spectra measured for the electrolytic solutions doped with TBATPB in the concentration range between 50 and 500 ppb. The dielectric spectra observed for the electrolytic cells have been analyzed by using the classical theory, and we have obtained an unrealistic result that the number density of ions in the cell becomes more than one order of magnitude larger than that of the doped ions [18]. Alexe-Ionescu and co-workers have criticized the approximation with the homogeneous field for the analysis of the space-charge polarization, and they have insisted that the assumption of the homogeneous field should lead to incorrect values of the ionic constants, such as the diffusion coefficient and the number density of ions [23]. On the other hand, they have analyzed the space-charge polarization just by using the classical theory, not by considering the contribution of the space-charge polarization to the dielectric constant of Poisson's equation. They have calculated the ionic constants performing a rescaling treatment with the classical theory against the values obtained by the homogeneous field approximation. From the above discussion, the values of the ionic constants obtained by the rescaling treatment should be far different from the correct values.

It is possible to calculate the complex dielectric constant due to the space-charge polarization under the correct internal field satisfying Poisson's equation considering the contribution of the space-charge polarization to the dielectric constant [9]. In this case, a numerical calculation has to be carried out because it is difficult to obtain an analytical solution of the PNP equation. It is too complicated to apply the numerical treatment to the present work, then, we assume here, with the recognition of a small error around 10% in terms of the Stokes radius, that the ac internal field at time t is homogeneous between the electrodes and is written as $E(t) = E_1 \exp(i\omega t)$ where $E_1 = V_1/d$.

By substituting the expressions of the form of Eq. (12) into Eqs. (5), (6), (10), and (11), we obtain

$$i\omega p_1(x) = D\, d^2 p_1(x)/dx^2, \tag{13}$$

$$i\omega n_1(x) = D\, d^2 n_1(x)/dx^2, \tag{14}$$

$$j_{p_1}(x) = q\mu c_0 E_1 - qD\, \partial p_1(x)/\partial x = 0 \,(\text{at } x = 0 \text{ and } d), \tag{15}$$

$$j_{n_1}(x) = q\mu c_0 E_1 + qD\, \partial n_1(x)/\partial x = 0 \,(\text{at } x = 0 \text{ and } d). \tag{16}$$

The solutions of Eqs. (13) and (14), under the boundary conditions of Eqs. (15) and (16), are represented by

$$p_1(x) = A_p \exp(zx) + B_p \exp(-zx), \tag{17}$$

and

$$n_1(x) = A_n \exp(zx) + B_n \exp(-zx), \tag{18}$$

respectively, where

$$A_p = \frac{\mu c_0 V_1}{dDZ}\left[\frac{1 - \exp(-Zd)}{\exp(Zd) - \exp(-Zd)}\right], \tag{19}$$

$$B_p = \frac{\mu c_0 V_1}{dDZ}\left[\frac{1 - \exp(Zd)}{\exp(Zd) - \exp(-Zd)}\right], \tag{20}$$

$$A_n = \frac{\mu c_0 V_1}{dDZ}\left[\frac{\exp(-Zd) - 1}{\exp(Zd) - \exp(-Zd)}\right], \tag{21}$$

$$B_n = \frac{\mu c_0 V_1}{dDZ}\left[\frac{\exp(Zd) - 1}{\exp(Zd) - \exp(-Zd)}\right], \tag{22}$$

where $Z = \sqrt{i\omega/D}$.

The current density within the solution layer is given by the sum of a displacement term and two transport terms arising from the motion of the positive and negative ions, and it is, thus, expressed as

$$j_1(x) = \varepsilon_0 \varepsilon_s d E(t)/dt + q[2\mu c_0 V_1/d - D\, dp_1(x)/dx + D\, dn_1(x)/dx]. \tag{23}$$

The total current density J_1 flowing into the solution layer can be obtained by taking a space average of $j_1(x)$ over the

whole layer, and we obtain

$$J_1 = i\omega\varepsilon_0\varepsilon_s V_1/d + q\{2\mu c_0 V_1/d - D\,[p_1(d) - p_1(0)]/d + D\,[n_1(d) - n_1(0)]/d\}. \quad (24)$$

From Eqs. (17)–(22) and (24), the admittance per unit area $Y_1 (= J_1/V_1)$ is expressed as

$$Y_1 = \frac{i\omega\varepsilon_0\varepsilon_s}{d} + \frac{q}{d}\left\{2\mu c_0 - \frac{2\mu c_0}{Zd}\left[\frac{\exp(Zd) + \exp(-Zd) - 2}{\exp(Zd) - \exp(-Zd)}\right]\right. + \left.\frac{2\mu c_0}{Zd}\left[\frac{2 - \exp(Zd) - \exp(-Zd)}{\exp(Zd) - \exp(-Zd)}\right]\right\}. \quad (25)$$

The parallel resistance per unit area $R_i(\omega)$ and the parallel capacitance per unit area $C_i(\omega)$, given by the sum of the space-charge capacitance and the geometrical capacitance, are written as $R_i(\omega) = 1/Y_1'$ and $C_i(\omega) = Y_1''/\omega$, respectively, providing that $Y_1 = Y_1' + iY_1''$. Thus, we obtain the complex dielectric constant $\varepsilon_i^*(\omega) = \varepsilon_i'(\omega) - i\varepsilon_i''(\omega)$, where

$$\varepsilon_i'(\omega) = \frac{dC_i(\omega)}{\varepsilon_0} = \frac{dY''}{\omega\varepsilon_0}, \quad (26)$$

and

$$\varepsilon_i''(\omega) = \frac{d}{\omega\varepsilon_0 R_i(\omega)} = \frac{dY_1'}{\omega\varepsilon_0}. \quad (27)$$

The dielectric constant and the dielectric loss factor, obtained by using Eqs. (26) and (27), lead to the same values as those calculated by using Eqs. (5) and (6), respectively, in Ref. [4] assuming two ion species which have the same diffusion coefficient, mobility, and number density.

B. Space-charge polarization in the presence of ionic adsorption on the electrode

The adsorption of ions on electrodes has been discussed in terms of the general electrochemical reaction process. Armstrong and Henderson have derived the admittance for the electrochemical reaction with an adsorbed intermediate [24]. In the calculation of the faradic current, they employed a Taylor series expansion to avoid the need for specific assumptions concerning adsorption isotherm and reaction orders. The Taylor series expansion was carried out to first order on the response to the perturbation with two variables: One was the concentration of the adsorbed intermediates on the electrode surface, and the other was the potential difference. In their approach, the perturbation for the potential difference may be valid for a supported system in which the ionic concentration is so high that the applied voltage is concentrated at the interfaces between the solution and the electrodes. The charge transfer occurs on or within about one molecular or ionic radius of the electrode. Nevertheless, the internal electric field generated by an external voltage application is distributed over the Helmholtz and diffuse double layers for which the distance from the surface of the electrode becomes several times of Debye lengths, and the Debye length becomes large as the ionic concentration decreases. In order to cope with this problem, especially for unsupported systems, Macdonald [25] and Francheschetti and Macdonald [26] have introduced another perturbation variable to the theory of Armstrong and Henderson, that is, the number density of ions on the electrode based on the Chang-Jaffe boundary condition [11]. In the boundary condition developed by Macdonald, it is implicitly assumed that the number of adsorption sites on the electrode is much larger than the number of ions to be adsorbed and the interaction between adsorbed ions can be neglected.

In the present model, we assume that the adsorption rate of the positive ions on the electrode is equal to that of the negative ions. According to the boundary condition by Macdonald [25], the current densities arising from the motion of the positive and negative ions at $x = 0$ and $x = d$ are expressed as

$$j_{p_1}(0) = q\mu c_0 E_1(0) - qD\,\partial p_1(0)/\partial x = -\xi^* q p_1(0), \quad (28)$$

$$j_{p_1}(d) = q\mu c_0 E_1(d) - qD\,\partial p_1(d)/\partial x = \xi^* q p_1(d), \quad (29)$$

$$j_{n_1}(0) = q\mu c_0 E_1(0) + qD\,\partial n_1(0)/\partial x = \xi^* q n_1(0), \quad (30)$$

$$j_{n_1}(d) = q\mu c_0 E_1(d) + qD\,\partial n_1(d)/\partial x = -\xi^* q n_1(d), \quad (31)$$

If no charge transfer occurs between the adsorbed ions and the electrode, ξ^* is written as

$$\xi^* = \xi' + i\xi'' = \frac{\omega^2\tau^2\xi_\infty}{1 + \omega^2\tau^2} + i\frac{\omega\tau\xi_\infty}{1 + \omega^2\tau^2}. \quad (32)$$

Assuming that the concentration of the positive or negative ions per unit area adsorbed on the electrode is Γ and the net rate of the adsorption of the positive or negative ions is v, it is defined that $\xi_\infty = (\partial v/\partial c_{s1})_\Gamma$, $\tau = -(\partial\Gamma/\partial v)_{c_{s1}}$, where c_{s1} represents the number density of the positive or negative ions at the surface of the electrode. The impedance spectrum of an electrolytic cell in the presence of ionic adsorption has also been analyzed by Barbero [19], introducing a kinetic equation composed of adsorption and desorption terms in accordance with a Langmuir isotherm. In the present paper, ξ_∞ and τ correspond to the adsorption and desorption constants, respectively. However, the analytical formula by Barbero [19] does not take account of the influence of external charges on the internal field formation, and thus, it cannot be used for the analysis of practical experimental data. Equations (28)–(32) are the same forms as those developed by Lányi [27]; nevertheless, his formalism for the boundary condition has not been developed in terms of the adsorption of ions on the electrode.

By substituting Eq. (15) with Eqs. (28) and (29) and substituting Eq. (16) with Eqs. (30) and (31), the solutions of Eqs. (13) and (14) are represented by

$$p_1(x) = A_{ap}\exp(zx) + B_{ap}\exp(-zx), \quad (33)$$

and

$$n_1(x) = A_{an}\exp(zx) + B_{an}\exp(-zx), \quad (34)$$

where

$$A_{ap} = \frac{\mu c_0 V_1}{d}\left[\frac{DZ + \xi^* - (DZ - \xi^*)\exp(-Zd)}{(DZ + \xi^*)^2\exp(Zd) - (DZ - \xi^*)^2\exp(-Zd)}\right], \quad (35)$$

$$B_{ap} = \frac{\mu c_0 V_1}{d}\left[\frac{DZ - \xi^* - (DZ + \xi^*)\exp(Zd)}{(DZ + \xi^*)^2 \exp(Zd) - (DZ - \xi^*)^2 \exp(-Zd)}\right], \tag{36}$$

$$A_{an} = \frac{\mu c_0 V_1}{d}\left[\frac{(DZ - \xi^*)\exp(-Zd) - DZ - \xi^*}{(DZ + \xi^*)^2 \exp(Zd) - (DZ - \xi^*)^2 \exp(-Zd)}\right], \tag{37}$$

$$B_{an} = \frac{\mu c_0 V_1}{d}\left[\frac{(DZ + \xi^*)\exp(Zd) - DZ + \xi^*}{(DZ + \xi^*)^2 \exp(Zd) - (DZ - \xi^*)^2 \exp(-Zd)}\right]. \tag{38}$$

By calculating the current density in a similar way to that in Sec. II A, the admittance per unit area Y_1 $\left(= Y_1' + iY_1''\right)$ is written as

$$Y_1 = \frac{i\omega\varepsilon_0\varepsilon_s}{d} + \frac{q}{d}\left(2\mu c_0 - \frac{D}{V_1}\{A_{ap}[\exp(Zd) - 1] + B_{ap}[\exp(-Zd) - 1]\} + \frac{D}{V_1}\{A_{an}[\exp(Zd) - 1] + B_{an}[\exp(-Zd) - 1]\}\right). \tag{39}$$

Finally, the dielectric constant $\varepsilon_i'(\omega)$ and the dielectric loss factor $\varepsilon_i''(\omega)$ are calculated using Eqs. (39), (26), and (27).

C. Simulation of the electrode polarization in the presence of ionic adsorption on the electrode

We will simulate the frequency dependence of the complex dielectric constant attributed to the electrode polarization in the presence of specific ionic adsorption by using Eqs. (39), (26), and (27). In the simulation, we set $D = 8.2 \times 10^{-10}$ m^2/s and $\mu = 3.2 \times 10^{-8}$m^2 V^{-1} s^{-1}. The frequency dependence of the complex dielectric constant calculated providing $c_0 = 1.2 \times 10^{20}$ m^{-3} and $\tau = 10$ s is shown in Fig. 1 with respect to different ξ_∞ values. In the absence of the ionic adsorption, the dielectric constant increases with decreasing frequency in the frequency range between 1 and 10^3 Hz and takes a constant value in the frequency range below 1 Hz. For $\xi_\infty = 10^{-6}$, 10^{-5}, and 10^{-4} m/s, another dielectric relaxation, that is due to the ionic adsorption, appears in the frequency range below 1 Hz in Fig. 1(a). The value at plateau in the dielectric constant in the lower-frequency region becomes large as ξ_∞ increases from 10^{-6} to 10^{-4} m/s, whereas, the value at plateau in the higher-frequency region, that is attributed to the space-charge polarization, becomes significantly small for $\xi_\infty = 10^{-4}$ m/s compared to those for $\xi_\infty = 10^{-6}$ and 10^{-5} m/s. From Fig. 1(b), it is found that the relaxation frequency that appeared in the lower-frequency region, at which the dielectric loss factor exhibits a maximum value, decreases slightly with an increasing ξ_∞ value.

The frequency dependence of the complex dielectric constant calculated providing $c_0 = 1.2 \times 10^{20}$ m^{-3} and $\xi_\infty = 10^{-5}$ m/s is shown in Fig. 2 with respect to different τ values. The value at plateau in the dielectric constant at the lower-frequency region becomes large as τ increases from 1 to 100 s, whereas, the value at plateau in the higher-frequency region is almost the same among the different τ values. From Fig. 2(b), it is found that the relaxation frequency that appeared in the lower-frequency region decreases proportionally with an increasing τ value.

The frequency dependence of the complex dielectric constant, calculated providing $\xi_\infty = 10^{-5}$ m/s and $\tau = 10$ s, is shown in Fig. 3 with respect to different c_0 values. In Fig. 3(a), the dielectric constants increase proportionally with an increasing c_0 value in the whole frequency range except for the range above 10 Hz where the contribution of dipole polarizations becomes dominant. In Fig. 3(b), the dielectric loss factors also increase proportionally with the increasing c_0 value. The relaxation frequencies for the two kinds of dielectric relaxations do not change with the c_0 value.

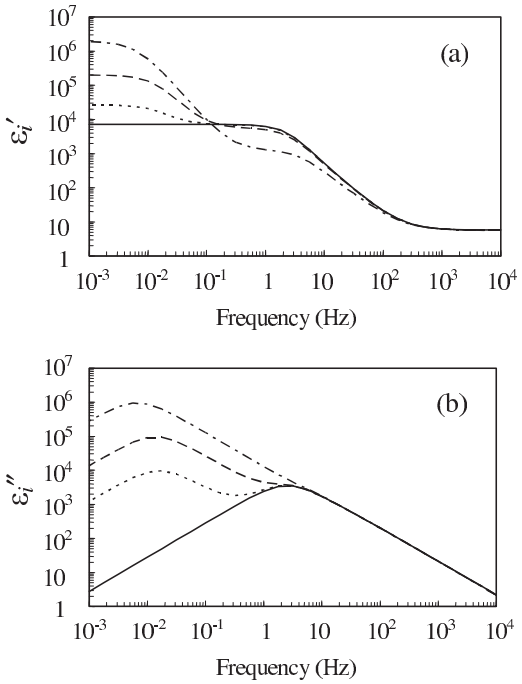

FIG. 1. Frequency dependence of (a) the dielectric constant and (b) the dielectric loss factor. The solid lines represent the values calculated in the absence of the adsorption of ions on the electrode. The dotted lines, dashed lines, and dot-dashed repeat lines represent the values calculated in the presence of the adsorption of ions with $\xi_\infty = 10^{-6}$, $\xi_\infty = 10^{-5}$, and $\xi_\infty = 10^{-4}$ m/s, respectively.

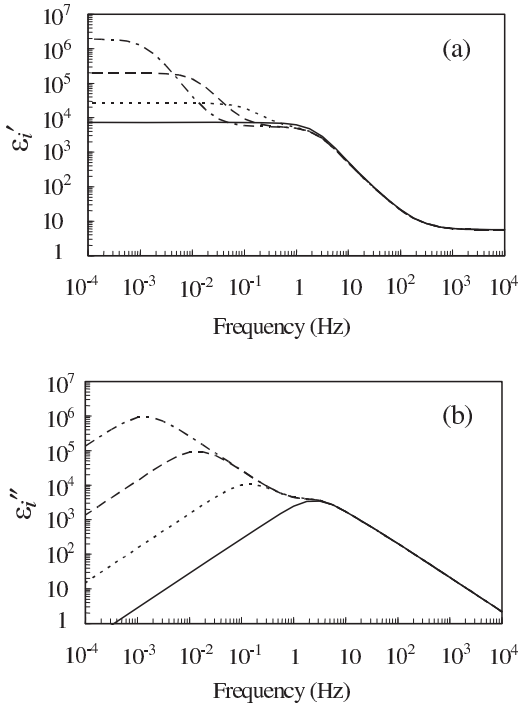

FIG. 2. Frequency dependence of (a) the dielectric constant and (b) the dielectric loss factor. The solid lines represent the values calculated in the absence of the adsorption of ions on the electrode. The dotted lines, dashed lines, and dot-dashed repeat lines represent the values calculated in the presence of the adsorption of ions with $\tau = 1$, $\tau = 10$, and $\tau = 100$ s, respectively.

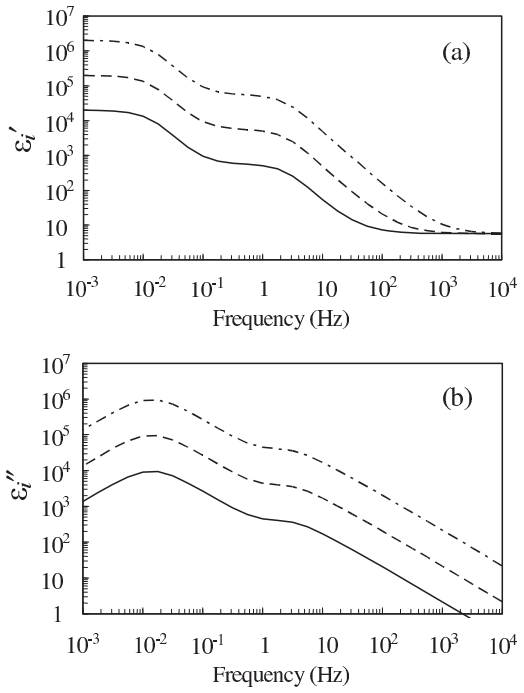

FIG. 3. Frequency dependence of (a) the dielectric constant and (b) the dielectric loss factor. The solid lines, dashed lines, and dot-dashed repeat lines represent the values calculated in the presence of the adsorption of ions with $c_0 = 1.2 \times 10^{19}$, $c_0 = 1.2 \times 10^{20}$, and $c_0 = 1.2 \times 10^{21}$ m^{-3}, respectively.

III. EXPERIMENT

Nine kinds of electrolyte solution samples were prepared using chlorobenzene (C_6H_5Cl) as a solvent and TBATPB as a solute in order to measure the complex dielectric constant in a low-frequency region. The concentrations of TBATPB doped into the solutions were 0, 50, 100, 200, 500 ppb, 1 ppm (parts per 10^6), 5, 10, and 50 ppm. These concentrations are equal to 0,8.9×10^{-8}, 1.8×10^{-7}, 3.6×10^{-7}, 8.9×10^{-7}, 1.8×10^{-6}, 8.9×10^{-6}, 1.8×10^{-5}, and 8.9×10^{-5} mol/l, respectively. These solution samples were injected into parallel-plate glass cells with indium tin oxide (ITO) electrodes, the area and distance between electrodes of which are 1.13 cm^2 and 22 μm, respectively. The impedance of the cell was measured using a Solartron 1260 frequency response analyzer connected to a 1296 current amplifier in the frequency range between 0.001 Hz and 10 KHz at 20 °C. The ac voltage applied to the cell was 5 mV (rms). The frequency dependences of the dielectric constant and the dielectric loss factor were calculated from the impedance value observed. The data for TBATPB concentrations of 0, 50, 100, 200, and 500 ppb are the same as those in the author's previous papers [17,18], and the measurements for 1, 5, 10, and 50 ppm were carried out together at that time.

The measurement of the complex dielectric constant for each dilute electrolytic cell was started within 10 min after injecting the solution into the cell. (It took around 5 min to obtain a stable temperature in an oven heated at 20 °C after setting the cell.) The measurement was started at 10^4 Hz and was ended at 10^{-3} Hz. For the impedance measurement, it takes about 90 s during 10^4 and 10^{-1} Hz, about 4.5 min during 10^4 and 10^{-2} Hz, and about 45 min during 10^4 and 10^{-3} Hz. It has been confirmed that it takes longer than several hours for TBA^+ or TPB^- ions to be adsorbed naturally on the ITO electrode in significant quantities [22]. Consequently, the change in the electrode potential due to the naturally adsorbed ions and the formation of the static diffuse double layer near the surface of the electrode should not significantly influence the frequency dependence of the complex dielectric constant of the electrolytic cell observed in the present measurement.

The frequency dependence of the relative dielectric constant and the relative dielectric loss factor observed for the electrolytic cells are shown in Figs. 4(a) and 4(b), respectively. In Fig. 4(a), the anomalous increase in the relative dielectric constant with decreasing frequency shows two relaxation phenomena for every cell. The first increase in the relative dielectric constant, observed in the frequency region between 10^{-1} and 10^3 Hz, is originated by the space-charge polarization attributed to the displacement of TBA^+ and TPB^- ions in the bulk layer under the influence of an external field. The plateau value in the relative dielectric constant due to the space-charge polarization increases as the TBATPB concentration becomes high. On the other hand, for the second dielectric relaxation that appeared in the lower-frequency region, the relative dielectric constant converges on a constant value at plateau regardless of the TBATPB concentrations. In Fig. 4(b), the relaxation frequency for the second dielectric relaxation, at which the relative dielectric loss factor exhibits the maximum value, shifts to the higher-frequency side as the TBATPB concentration becomes high.

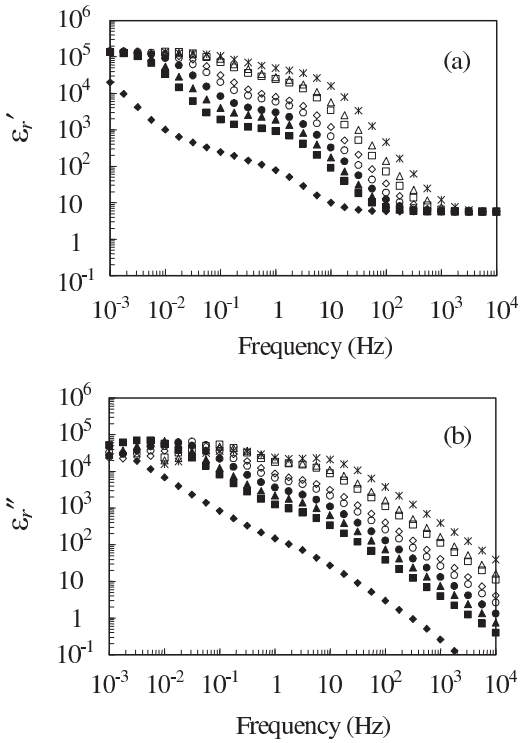

FIG. 4. Frequency dependence of the complex dielectric constant observed for chlorobenzene doped with TBATPB at different concentrations. ♦: 0 ppb; ■: 50 ppb; ▲: 100 ppb; •: 200 ppb; ○: 500 ppb; ◊: 1 ppm; □: 5 ppm; △: 10 ppm; and ∗: 50 ppm. The symbols in (a) represent the relative dielectric constants, whereas, those in (b) represent the relative dielectric loss factors.

IV. DATA ANALYSIS

As the two dielectric relaxations are observed in Fig. 4 for every chlorobenzene solution doped with TBATPB at different concentrations, the simulation result obtained in Sec. II suggests that the dielectric relaxation in the lower-frequency region may be induced by the ionic adsorption on the electrode. However, the dielectric constants in the lower-frequency region increase proportionally with increasing the number density of ions in the simulation result shown in Fig. 3, whereas, the dielectric constant at plateau in the lower-frequency region in Fig. 4(a) converges on a constant value regardless of the concentration of TBATPB, and the relaxation frequency shifts to the higher-frequency side with increasing the concentration of TBATPB as shown in Fig. 4(b).

It is known that TBATPB does not undergo solvation with any organic solvent molecule and the Stokes radii of TBA^+ and TPB^- are nearly the same [28,29]. The diffusion coefficient and the mobility of the TBA^+ ion are then nearly equal to those of the TPB^- ion, respectively, in the chlorobenzene solution. It was first shown by Grahame [30] that only negative ions were adsorbed on metal electrodes, and after that, it was found that tetra-alkyl ammonium cations could also be adsorbed on the metal electrode [31]. The author has shown that the TBA^+ and TPB^- ions are adsorbed naturally on ITO electrodes with different adsorption rates in the absence of an external field [22]. The result in Fig. 4 indicates that the increase in the capacitance due to the adsorption of TBA^+ and TPB^- ions on the ITO electrodes is restricted for some reason. The frequency-dependent behavior in the dielectric constant and the dielectric loss factor observed in Fig. 4 can be reproduced by using an equivalent circuit given in Fig. 5. $C_i(\omega)$ and $R_i(\omega)$ are calculated using Eqs. (39), (26), and (27), respectively. C_e in Fig. 5 represents the electrode capacitance, and the physical sense will be discussed in Sec. V.

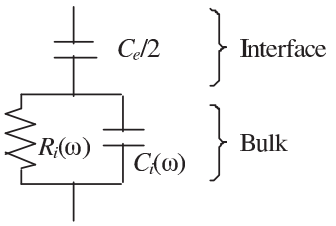

FIG. 5. Equivalent circuit of a dilute electrolytic cell in the presence of specific ionic adsorption.

In the previous paper, it has been shown that the relaxation frequency attributed to the space-charge polarization shifts to the lower-frequency side with the passage of time after filling the cell with the chlorobenzene doped with TBATPB at 100 ppb, and this phenomenon is interpreted by the change in electrode potential and the generation of static diffuse double layers on the electrodes that are caused by the adsorption of TBA^+ and TPB^- ions on the electrodes with different adsorption rates [22]. If the number densities of TBA^+ and TPB^- ions given in Table II of Ref. [22] are plotted with respect to the time in a graph and their relationship is analyzed by means of curve fitting using equations as $p = p_0(1 - t/\tau_p)$ and $n = n_0(1 - t/\tau_n)$, we obtain $\tau_p = 2.4 \times 10^4$ and $\tau_n = 2.0 \times 10^4$ s for the time constants of TBA^+ and TPB^-, respectively, that represent the decreasing rates of the bulk ion densities.

Since the measurements of the complex dielectric constant in Sec. III are started within 10 min after filling the cells with the chlorobenzene solutions, the data obtained in Fig. 4 represent the states before establishing an equilibrium in the absence of an external field. On the other hand, Eqs. (26) and (27), in connection with Eq. (39), are obtained by calculating the response to a small perturbation around the equilibrium. Here, the ions, preadsorbed on the electrode before establishing the equilibrium, do not affect the calculation because it is assumed that the surface number density of the preadsorbed ions is very small compared to the number density of the adsorption sites on the electrode and the interaction between the preadsorbed ions can be neglected. Besides, the positive or negative ions are adsorbed on the two plate electrodes with the same rate in the absence of the external voltage application. The magnitude of the current density, arising from the adsorption of the positive or negative ions to one electrode, is the same as that to the other electrode, and the direction of the current density at one electrode is opposite to that at the other electrode; therefore, no electric current appears in the external circuit. Moreover, the measurements in Sec. III are completed within 1 h after filling the cells with the chlorobenzene solutions, and the measurement time is much smaller than the value of τ_p or τ_n. From these conditions, the data in Fig. 4 may be analyzed using Eqs. (26) and (27) in connection with Eq. (39).

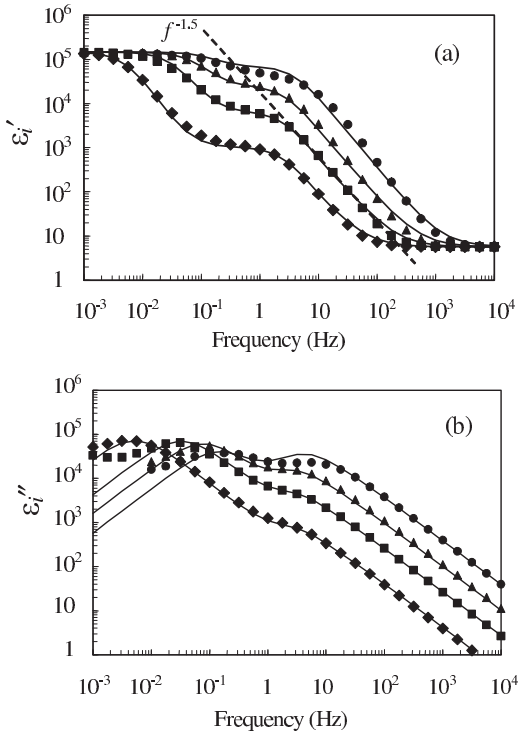

FIG. 6. Frequency dependence of (a) the dielectric constant and (b) the dielectric loss factor in the presence of ionic adsorption. The symbols represent observed values with ♦: 50 ppb; ■: 500 ppb; ▲: 5 ppm; and •: 50 ppm. The solid lines represent calculated values fitted to each concentration. The dashed line in (a) represents a slope of -1.5.

We assume that the Einstein relation is valid between the diffusion coefficient and the mobility, then $\mu = qD/(kT)$. From Figs. 1 and 2, it is found that the relaxation frequency in the lower-frequency region is determined dominantly by τ rather than ξ_∞. In Fig. 2, the frequency dependence of the complex dielectric constant is simulated in the range of τ between 1 and 100 s. On the other hand, because both values of τ_p and τ_n are much larger, it is presumed accordingly that the relaxation frequency depending on the TBATPB concentration observed in Fig. 4 is not determined by τ but is controlled by the presence of the electrode capacitance C_e given in Fig. 5. We then assume that $\tau = 2.0 \times 10^4$ s. With these preliminary findings, the fitting parameters to be determined are D, c, ξ_∞, and C_e.

The results of the curve fitting for the chlorobenzene samples doped with TBATPB at 50, 500 ppb, 5, and 50 ppm are shown in Fig. 6. The parameters determined by the curve fitting are listed in Table I. From Fig. 6, it is found that the dielectric constants and the dielectric loss factors observed for the four solutions are all well fitted by calculated values. In Table I, we obtain the same value of $D = 7.5 \times 10^{-10}$ m^2/s for all solutions. The Stokes radius r_s is calculated to be 3.6 Å by using the Stokes-Einstein equation providing the viscosity of chlorobenzene 0.799×10^{-3} Pa s, and this value is fairly close to the values for TBA^+ (3.8 Å) and TPB^- (4.1 Å) measured by means of conductmetry [28,29]. The TBATPB doping concentrations 50, 500 ppb, 5, and 50 ppm correspond to the number densities per unit volume 5.36×10^{19}, 5.36×10^{20}, 5.36×10^{21}, and 5.36×10^{22} m^{-3}, respectively. The number density of ion c_0 becomes large as the doping concentration is increased. Assuming that the number density of TBATPB doped per unit volume is a, the ratios of c_0 to a become 0.47, 0.30, 0.11, and 0.043, respectively. The decrease in the ratio indicates that the number of ion pairs by TBA^+ and TPB^- increases in the chlorobenzene solution with increasing the doping concentration. The adsorption constant ξ_∞, obtained for the 50 ppb solution, is the same as that for the 500 ppb solution, but the value becomes smaller with higher doping concentrations. The value at plateau in the dielectric constant in the lower-frequency region for all the solutions is determined by the capacitance C_e given in Fig. 5. The value of the capacitance 1.3×10^{-5} F, obtained for all the samples, is calculated to be 1.15×10^{-5} F/cm^2 for the capacitance per unit area.

V. DISCUSSION

The generation of a dipole potential or an interfacial capacitance between the electrode and the Helmholtz layer has been explained by several researchers introducing the jellium model that formulates the electronic structure of a metal electrode surface [32–35]. In the jellium model, the ionic charge is represented by a constant positive background charge, which drops abruptly to zero at the metal surface (jellium edge), whereas, the electrons are modeled as an inhomogeneous electron gas, which interacts with the positive background [20]. The electronic density shows the relatively slow decay at the metal surface, and the decay profile entails a small but appreciable negative charge density on the outside of the surface. This is known as the electronic spillover. The small amount of the negative charge density is balanced by a positive excess charge on the inside, then this charge distribution gives rise to a surface dipole potential [36].

The electrons on the outside of the surface interact with an external electric field. A positive charge on the metal surface pulls the electrons back into the metal; conversely, a negative charge pushes the electrons toward the solution. Amokrane and

TABLE I. Parameters determined by analyzing the complex dielectric constant of chlorobenzene solution doped with TBATPB.

Concentration of TBATPB	Diffusion coefficient D (m^2/s)	Number density c_0 (m^{-3})	Adsorption rate ξ_∞ (m/s)	Electrode capacitance C_e (F)
50 ppb	7.5×10^{-10}	2.5×10^{19}	1.5×10^{-5}	1.3×10^{-5}
500 ppb	7.5×10^{-10}	1.6×10^{20}	1.5×10^{-5}	1.3×10^{-5}
5 ppm	7.5×10^{-10}	6.0×10^{20}	1.0×10^{-5}	1.3×10^{-5}
50 ppm	7.5×10^{-10}	2.3×10^{21}	7.0×10^{-6}	1.3×10^{-5}

Badiali have suggested that the interaction between the metal dipole and the charge of the metal in the absence of specific ionic adsorption controls the distance of the closest approach of solvent molecules to the metal surface, and thus, the metal electrode capacitance C_e is generated by the variation in the distance [21,37]. According to their model, assuming that the solvent capacitance is C_s, the Helmholtz layer capacitance C_H is represented by two contributions in the series connection: $(C_H)^{-1} = (C_e)^{-1} + (C_s)^{-1}$. Since we are considering the dilute electrolytic cells in the presence of the specific ionic adsorption on the electrode, we cannot utilize the model of Amokrane and Badiali for the calculation of C_e in Fig. 6. Nevertheless, the concept of the metal capacitance should be valid even for the present electrochemical system, and the frequency-dependent behavior of the dielectric constant and dielectric loss factor, observed in Fig. 4, may be explained by using the equivalent circuit given in Fig. 5, incorporating the contribution of the electrode capacitance. Here, the presence of C_s is neglected in the equivalent circuit in Fig. 5 assuming that its value is large enough compared to the value of C_e. If the value of C_s is comparable or smaller than that of C_e, the influence of C_s has to be considered in the theoretical calculation in Sec. II B.

The negative slope of the dielectric constant increasing with frequency becomes -1.5 for the contribution of the space-charge polarization [4,22], and in Fig. 6, it is demonstrated for the solution in which TBATPB is doped at 500 ppb. The absolute value of the slope increases with increasing the TBATPB concentration in the range over 1 ppm due to the contribution of C_e. If we simulate the frequency dependence of the dielectric constant for the concentrations much higher than 50 ppm, we find that the value of the slope approaches -2. For such high electrolyte concentrations, the contributions of the space-charge polarization and the specific ionic adsorption on the dielectric constant are both suppressed largely by the metal capacitance, and thus, the Debye-type dielectric relaxation is observed. The Debye-type dielectric relaxation may be analyzed by applying a classical model composed of the Helmholtz layer capacitance, the diffuse double layer capacitance, and the bulk solution layer resistance in series combination, but it should be emphasized that the origin of the Debye-type dielectric relaxation may include more complicated factors as shown in the present paper. On the other hand, in the case that the concentration of mobile ions is sufficiently low and the electrode capacitance is much larger than the capacitance arising from the space-charge polarization, the space-charge polarization can be analyzed neglecting the influence of the electrode capacitance. Although the space-charge polarization for electrolytic cells is generally analyzed by using the Poisson-Nernst-Planck equation, an accurate discussion can be conducted only in such a condition.

VI. CONCLUSION

We observed two kinds of dielectric relaxations in low-frequency regions for dilute electrolytic cells filled with chlorobenzene doped with TBATPB at different concentrations. The dielectric relaxation at the higher-frequency region is due to the contribution of the space-charge polarization attributed to TBA^+ and TPB^- ions dissociated in the bulk layer, and another anomalous increase in the dielectric constant that appeared at lower frequencies is induced by the specific adsorption of TBA^+ and TPB^- ions on the electrodes. The dielectric constant at the low frequencies converged on a constant value regardless of the TBATPB concentrations. This upper limit of the dielectric constant appears due to the fact that the closest distance that the ions can approach the electrode is restricted by an electronic spillover from the electrode surface. The new model of the electrode polarization, developed in the present paper, can be expressed with a simple equivalent circuit that consists of the space-charge polarization accompanied by a specific ionic adsorption and a series capacitance brought about by the electronic structure of the electrode surface. The frequency-dependent dielectric behavior, observed for the dilute electrolytic cells, can primarily be explained by the new model regardless of the concentration of the electrolyte.

ACKNOWLEDGMENT

The author is grateful to Dr. S. Naemura, the Visiting Professor of University of Southampton, for helpful discussions.

[1] S. Uemura, J. Polym. Sci., Polym. Phys. Ed. **10**, 2155 (1972).
[2] S. Uemura, J. Polym. Sci., Polym. Phys. Ed. **12**, 1177 (1974).
[3] S. Murakami and H. Naito, Jpn. J. Appl. Phys. **36**, 2222 (1997).
[4] A. Sawada, K. Tarumi, and S. Naemura, Jpn. J. Appl. Phys. **38**, 1418 (1999).
[5] S. Dhara and N. V. Madhusudana, J. Appl. Phys. **90**, 3483 (2001).
[6] Y. Huang, A. Bhowmik, and P. J. Bos, Jpn. J. Appl. Phys. **51**, 031701 (2012).
[7] M. Mackey, D. E. Schuele, L. Zhu, and E. Baer, J. Appl. Phys. **111**, 113702 (2012).
[8] R. Coelho, Rev. Phys. Appl. **18**, 137 (1983).
[9] A. Sawada, J. Chem. Phys. **129**, 064701 (2008).
[10] G. Jaffé, Phys. Rev. **85**, 354 (1952).
[11] H. Chang and G. Jaffé, J. Chem. Phys. **20**, 1071 (1952).
[12] J. R. Macdonald, Phys. Rev. **92**, 4 (1953).
[13] R. Friauf, J. Chem. Phys. **22**, 1329 (1954).
[14] M. Z. Bazant, K. Thornton, and A. Ajdari, Phys. Rev. E **70**, 021506 (2004).
[15] Y. Y. Wang, C.-N. Sun, F. Fan, J. R. Sangoro, M. B. Berman, S. G. Greenbaum, T. A. Zawodzinski, and A. P. Sokolov, Phys. Rev. E **87**, 042308 (2013).
[16] A. Sawada, H. Sato, A. Manabe, and S. Naemura, Jpn. J. Appl. Phys. **39**, 3496 (2000).
[17] A. Sawada, J. Appl. Phys. **100**, 074103 (2006).
[18] A. Sawada, J. Chem. Phys. **126**, 224515 (2007).
[19] G. Barbero, Phys. Rev. E **71**, 062201 (2005).
[20] N. D. Lang and W. Kohn, Phys. Rev. B **1**, 4555 (1970); **3**, 1215 (1971).
[21] S. Amokrane and J. P. Badiali, J. Electroanal. Chem. **266**, 21 (1989).

[22] A. Sawada, J. Appl. Phys. **112**, 044104 (2012).
[23] A. L. Alexe-Ionescu, G. Barbero, and I. Lelidis, Phys. Rev. E **80**, 061203 (2009).
[24] R. D. Armstrong and M. Henderson, J. Electroanal. Chem. **39**, 81 (1972).
[25] J. R. Macdonald, J. Electroanal. Chem. **70**, 17 (1976).
[26] D. R. Franceschetti and J. R. Macdonald, J. Electroanal. Chem. **82**, 271 (1977).
[27] Š. Lányi, J. Phys. Chem. Solids **36**, 775 (1975).
[28] R. M. Fuoss and E. Hirsch, J. Am. Chem. Soc. **82**, 1013 (1960).
[29] B. S. Krumgalz, J. Chem. Soc., Faraday Trans. 1 **78**, 437 (1982).
[30] D. C. Grahame, Chem. Rev. **41**, 441 (1947).
[31] M. A. V. Devanathan and M. J. Fernando, Trans. Faraday Soc. **58**, 368 (1962).
[32] J. P. Badiali and M. L. Rosinberg, J. Electroanal. Chem. **150**, 25 (1983).
[33] W. Schmickler and D. Henderson, J. Electroanal. Chem. **176**, 383 (1984).
[34] A. A. Kornyshev and M. A. Vorotyntsev, J. Electroanal. Chem. **167**, 1 (1984).
[35] J. W. Halley, B. Johnson, D. Price, and M. Schwalm, Phys. Rev. B **31**, 7695 (1985).
[36] W. Schmickler, Chem. Rev. **96**, 3177 (1996).
[37] S. Amokrane and J. P. Badiali, Electrochim. Acta **34**, 39 (1989).